Parameter boundaries for the heteroepitaxial growth of REBCO films by e-beam quantitative evaporation on inclined substrate deposited MgO buffered Hastelloy tapes

Journal of Physics: Conference Series **1559** (2020) 012035 doi:10.1088/1742-6596/1559/1/012035

Parameter boundaries for the heteroepitaxial growth of REBCO films by e-beam quantitative evaporation on inclined substrate deposited MgO buffered Hastelloy tapes

Oleksiy Troshyn[1], Christian Hoffmann[2], Veit Große[1], Jens Hänisch[3] and Bernhard Holzapfel[3]

[1]THEVA Dünnschichttechnik GmbH, Rote-Kreuz-Str. 8, 85737 Ismaning, Germany
[2]Ceraco Ceramic Coating GmbH, Rote-Kreuz-Str. 8, 85737 Ismaning, Germany
[3]Institute for Technical Physics, Karlsruhe Institute of Technology (KIT), PO Box 36 40, 76021 Karlsruhe, Germany

troshyn@theva.com

Abstract. The technology of electron beam (e-beam) quantitative evaporation of oxide powders at THEVA is quite unique among the many standard in-situ growth methods of high-temperature superconducting (HTS) films. As well known for $YBa_2Cu_3O_{7-x}$ (YBCO) film growth the temperature and oxygen pressure should be in proximity of the YBCO stability line in the Bormann diagram. In case of e-beam quantitative evaporation, we observe a shift in the $DyBa_2Cu_3O_{7-x}$ (DyBCO) stability line towards lower pressures and higher temperatures compared to YBCO. We investigated the temperature and oxygen partial pressure boundaries of epitaxial DyBCO growth on inclined substrate deposited MgO (ISD-MgO) buffered Hastelloy tapes. For completeness, the influence of powder stoichiometry and evaporation rate on HTS epitaxial growth is shown. For the first time high-quality HTS films have been grown by e-beam quantitative evaporation without employing an oxygen shuttle and with oxygen in the chamber background instead.

1. Introduction

The quantitative evaporation of $REBa_2Cu_3O_{7-x}$ (REBCO, RE = Y, Dy, Gd) oxide powder by an electron beam is an established process used by THEVA for the deposition of high-quality HTS films on metal tapes. While processing the tapes are moving through a deposition area of 20 × 40 cm^2 and the film growth takes place at an oxygen partial pressure of 1×10^{-4} mbar and a substrate temperature of around 700˚C. According to the Bormann diagram [1, 2] the REBCO superconductor is not stable under these conditions. To stabilize REBCO and oxidize the deposited thin film, an oxygen shuttle with a frequency of 3-5 Hz moves linearly underneath the tapes in the deposition zone providing a periodic local O_2 pressure at the substrate of around 5×10^{-3} mbar [3]. The oxidation frequency is selected depending on the evaporation rate, so that almost every monolayer of condensed particles is oxidized by an oxygen shower [4].

The oxygen shuttle has several disadvantages. The linear motion of the shuttle is realized through a complex mechanical design, which reduces the reliability of long-term deposition and whose maintenance is time consuming. Moreover, the sample surface is partially shaded by the shuttle thus reducing the efficiency of using the expensive REBCO powder.

To eliminate the mentioned drawbacks and increase the reliability of the entire system, HTS growth without an oxygen shuttle and with oxygen in the chamber background instead is of great interest. A first indication of the feasibility of such an approach can be found in ref. [5], where YBCO was deposited using two different techniques, namely thermal co-evaporation of metals and quantitative evaporation of YBCO oxide powder. The evaporation rate in both cases was measured by atomic absorption spectroscopy. The lines of Y, Ba, and Cu were detected during thermal co-evaporation of metals, while only the line of Cu was detected during the electron beam evaporation of the YBCO powder. This indicates that in the latter case yttrium and barium-containing particles were vaporized in the oxidized form. For the formation of the structurally stable YBCO phase a high O_2 pressure may therefore not be required.

Since deposition temperature, deposition rate and stoichiometry at a given oxygen partial pressure are interrelated, their boundaries with regard to epitaxial growth of HTS thin films will be investigated. DyBCO and GdBCO are used as representatives for the class of REBCO-based superconductors.

2. Experiment

2.1. Deposition system

REBCO powder with a grain size of <0.5 mm was evaporated by quantitative electron beam evaporation on a Hastelloy/ISD-MgO/MgO - cap layer architecture, described in detail elsewhere [3]. Briefly, REBCO powder is continuously extracted from a funnel in form of a track and delivered to an e-beam evaporation spot by a rotating copper turntable. The evaporation rate was controlled by a quartz crystal monitor. The distance between the evaporation source and the substrate was 35 cm. Oxygen was supplied to the chamber at its background. The substrates located in the ceramic holder were heated by a radiation heater from the rear.

2.2. Temperature measurement

A contactless and accurate measurement of the substrate temperature during evaporation is very sophisticated. A practical and sufficiently accurate method (error 2%) to determine the substrate temperature is calibrating the sample temperature against the total heater power. In a preliminary experiment, a thermocouple was spot-welded to the sample and the temperature of the tape depending on the power of heaters was measured (see Table 1). Good reproducibility can be achieved when the reflectivity of the samples backside is kept constant.

Table 1. Substrate temperature versus heater power.

Total heater power (W)	Substrate temperature (°C)
1000	530
1500	620
2000	685
2500	750

2.3. Deposition parameters

For DyBCO thin film deposition, the substrate temperature was varied in the range from 530°C to 750°C at three different oxygen pressures: 1×10^{-4} mbar, 5×10^{-4} mbar and 1×10^{-3} mbar, the evaporation rate was varied from 1 Å/s to 3 Å/s. The powder stoichiometry of Dy:Ba:Cu = 20:25:55 was used for film depositions. The thickness of the DyBCO films was 220 nm.

2.4. Measurements

Sample surface morphology was analyzed by scanning electron microscopy (SEM) and sample stoichiometry by inductively coupled plasma mass spectroscopy. The J_c of the samples was measured inductively (77 K, self-field) with a setup described in ref. [6].

3. Results

3.1. Dependence of film growth on oxygen partial pressure and substrate temperature

The critical current density of the DyBCO films within the above-mentioned parameter field is shown in Fig. 1. All films deposited at $P(O_2) = 1 \times 10^{-4}$ mbar within the entire temperature range are not superconducting. The same is true for all DyBCO films that were deposited at the substrate temperature of 530°C and 750°C resulting in the boundary conditions for DyBCO film growth: 530°C < T < 750°C and an oxygen partial pressure of $P(O_2) > 1 \times 10^{-4}$ mbar. Superconducting films with a critical current density of around 0.3 MA/cm² were obtained at higher pressures and in the temperature range of 620°C to 685°C.

The influence of the substrate temperature on the surface morphology of the films follows a general pattern and therefore only samples deposited at an oxygen pressure of 1×10^{-3} mbar will be considered in more detail (Fig. 2a-d). All samples, except those grown at 750°C, consist of smooth terraces/tiles with distinct edges and vertices pointing down and reproduce therefore the morphology of the underlying MgO buffer layer.

A film grown at 530°C consists of many misoriented crystallites which originate from insufficient surface diffusion of particles at this temperature. With increasing the temperature from 530˚C to 685˚C, the surface diffusion length of adsorbed particles also increases. As a result, the number of particles embedded in energetically favorable positions, kink and step sites, grows. Consequently, the number of misorientations and defects in the crystal decreases, thus explaining the increase of the critical current density from 0 to 0.27 mA/cm^2 in the temperature range from 530°C to 685°C. Also due to enhanced particle surface diffusion, small terraces grow together into larger ones, thereby reducing their total number.

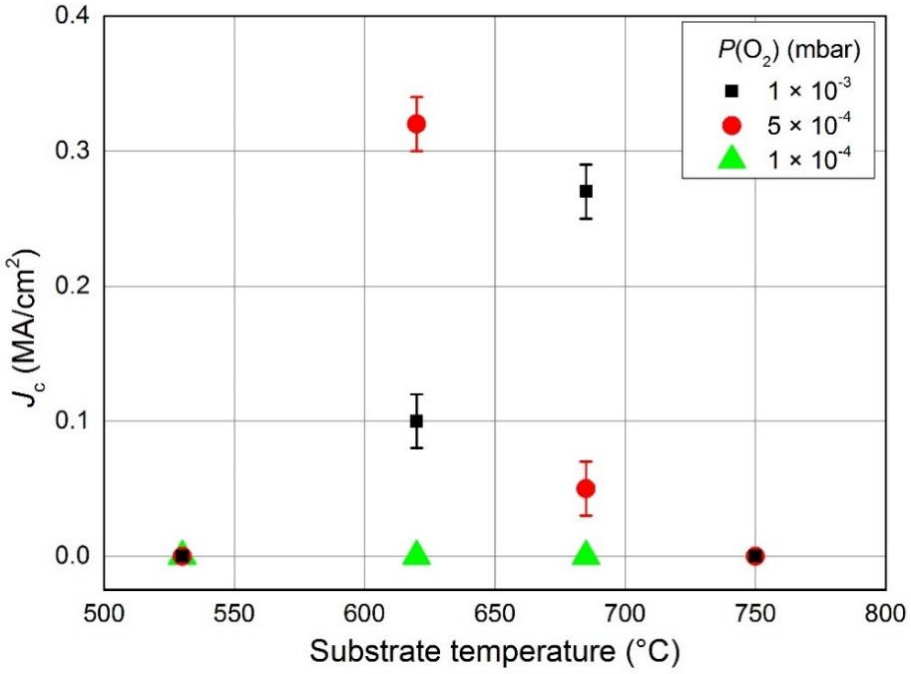

Figure 1. The critical current density of DyBCO films grown in a large temperature vs. oxygen partial pressure parameter range.

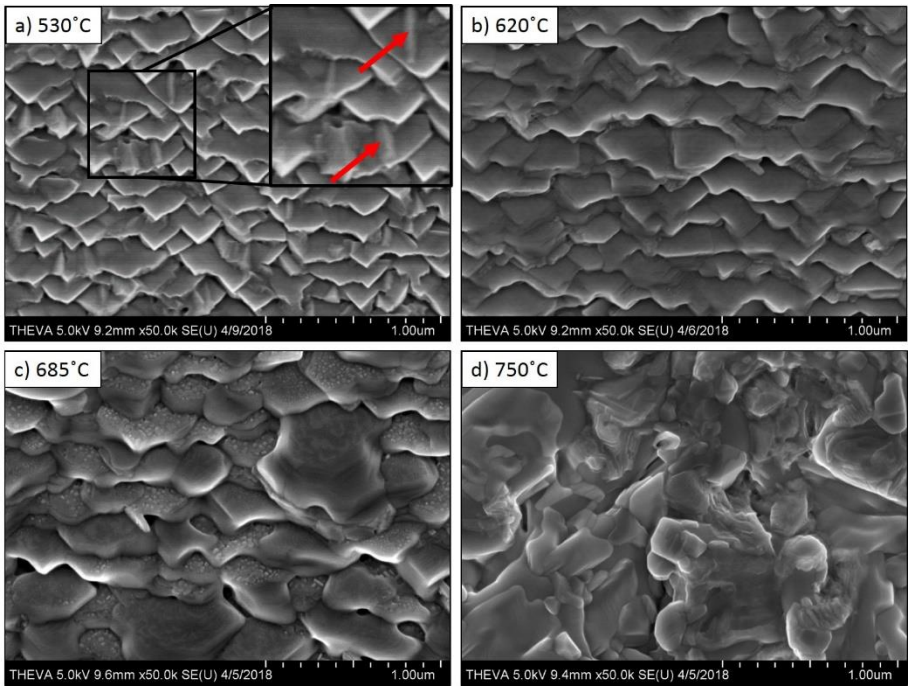

Figure 2. Surface morphology of DyBCO films deposited at an oxygen partial pressure of 1×10^{-3} mbar at different substrate temperatures. Red arrows in the insert (a) mark misoriented crystallites. Images were recorded with the secondary electrons detector at a SEM.

The morphology of the DyBCO film grown at 750°C does not show characteristic terraces. In addition, at this temperature the DyBCO decomposes into various phases as can be seen on SEM images using the backscattered electron detector (BSE). While the surface of the sample obtained at 685°C consists of sections with different gray tones with smooth transition between them, the film deposited at T = 750°C consists of two areas of different colors with sharp boundaries in between (Fig. 3a, b). This indicates the formation of at least two phases and is consistent with phase diagrams from literature. At high temperatures, the DyBCO phase decomposes according to the following reaction [1]:

$$2\ DyBa_2Cu_3O_7 = Dy_2BaCuO_5 + 3\ BaCuO_2 + Cu_2O + O_2$$

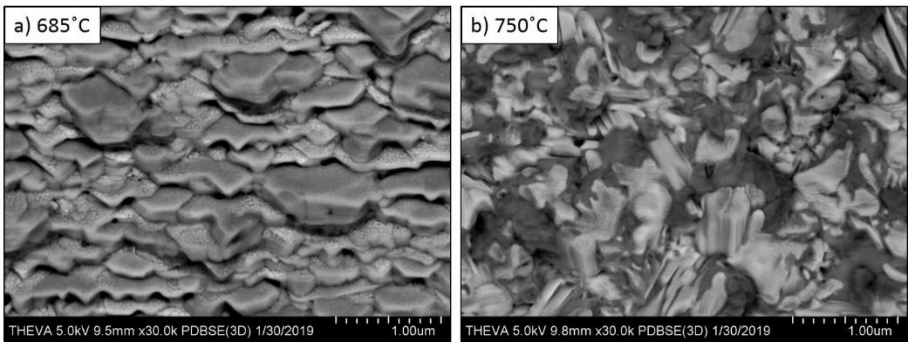

Figure 3. Surface morphology of DyBCO films deposited at $P(O_2)$ = 1×10^{-3} mbar and temperatures of a) 685°C and b) 750°C, recorded using a BSE detector. Areas of two colors with sharp boundaries in between indicate two phases.

The stability regions of YBCO and DyBCO regarding oxygen partial pressure and substrate temperature are shown in detail in the Hammond and Bormann phase diagram in Fig. 4d. With our data, the stability line of the DyBCO film can be generated by slightly shifting the stability line of the tetragonal YBCO phase to the left, i.e. towards higher temperatures. This resulting DyBCO stability line is consistent with the published REBCO phase diagram corrections when replacing the rare-earth element with one of a larger ion radius [7].

A comparable decomposition of DyBCO films can be observed when varying the oxygen partial pressure at a given substrate temperature of 685°C, as shown in Fig. 4c. While the sample grown at an oxygen partial pressure of 1×10^{-3} mbar has a regular and crystalline tile morphology, the DyBCO phase of the film deposited at 1×10^{-4} mbar oxygen is completely decomposed. The third sample deposited at an intermediate oxygen partial pressure of 5×10^{-4} mbar consists of large areas with terraces but already shows regions with decomposed DyBCO. The observed morphological changes induced by lowering the oxygen partial pressure indicate a gradual increase of secondary phases in the DyBCO film and are responsible for the observed decrease of J_c (Fig. 1).

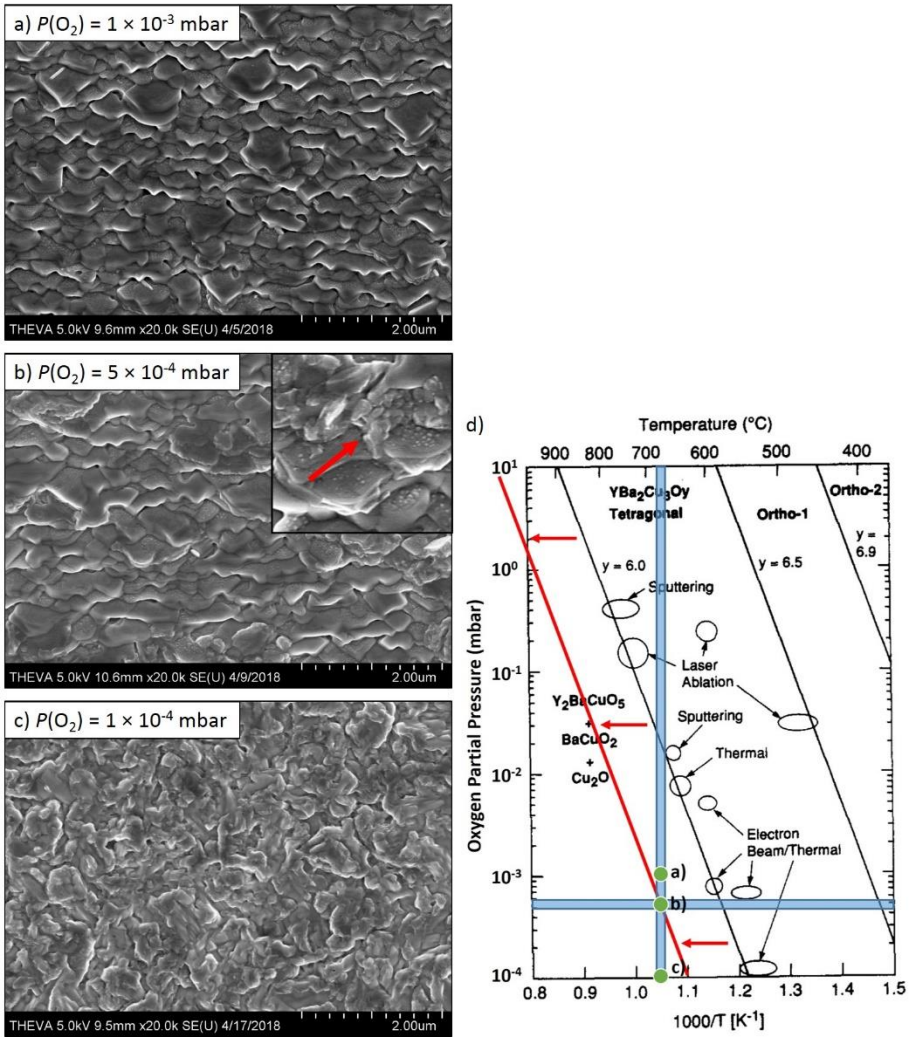

Figure 4. a)-c) Surface morphology of DyBCO films deposited at a substrate temperature of 685˚C and various oxygen partial pressures. The red arrow in the insert (b) marks a region of decomposed DyBCO. d) Phase stability diagram according to Hammond and Bormann [1]. The red line is the shifted phase stability line for the tetragonal $DyBa_2Cu_3O_{7-x}$ phase. The green dots indicate the growth conditions of the films shown in a) -c).

3.2. Influence of the deposition rate on the film growth

Besides the state variables temperature and oxygen pressure, the deposition rate also has an impact on the electrical properties of the DyBCO films. As the diffusion length of adsorbed molecules is inversely proportional to the deposition rate, the crystalline properties of the films should change with varying rates. Based on the optimal deposition conditions (1×10^{-3} mbar, 685°C), the evaporation rate was gradually increased from 1 Å/s via 2 Å/s to 3 Å/s. As expected, misorientations develop with increasing deposition rate and the density of these misoriented grains grows accordingly (Fig. 5). Although the films showed a critical temperature T_c of 83 K at 2 Å/s and 81 K at 3 Å/s a measurable critical current density vanished in films grown at 2 Å/s already.

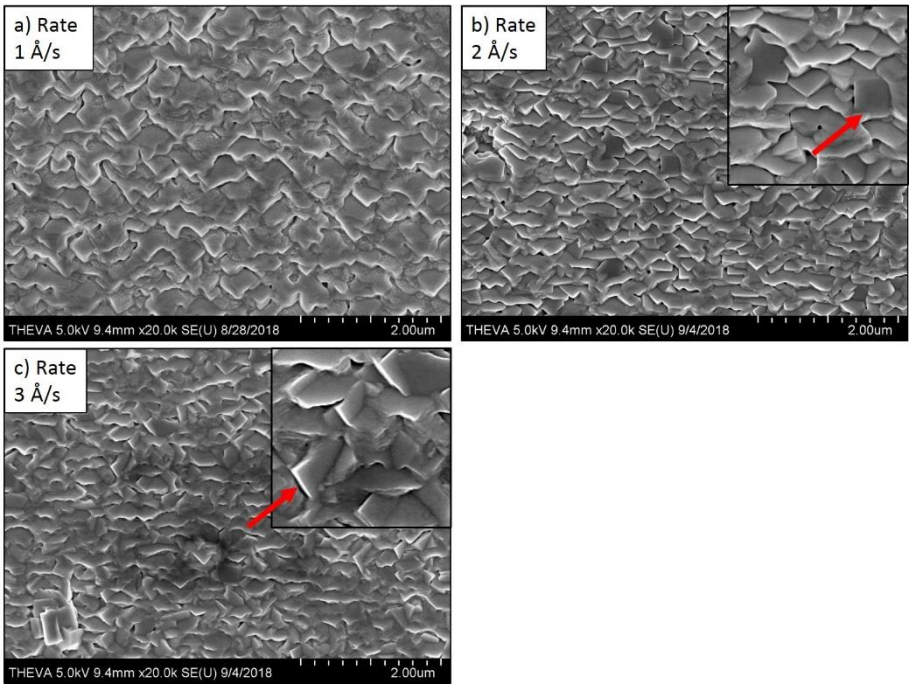

Figure 5. The SEM images of the DyBCO films deposited at various evaporation rates. The misorientations are marked with red arrows.

3.3. Dependence of the critical current density on film stoichiometry

The size of the stoichiometry region for the formation of films with high J_c is of particular interest in order to use e-beam evaporation of HTS-powder for the deposition on large areas. For manufacturing, only a large deposition area (e.g. 20 × 20 cm²) is economically attractive [8], and due to the nature of the evaporation method a composition distribution across such a large deposition area will unavoidably be present.

For these experiments, GdBCO powders were used to vary the precursor stoichiometry over a wide range since a choice of powders with varying composition were readily available. At the same time, the optimal deposition parameters of DyBCO are suitable for the growth of GdBCO since the stability line of GdBCO is shifted towards even higher temperatures compared to DyBCO [7].

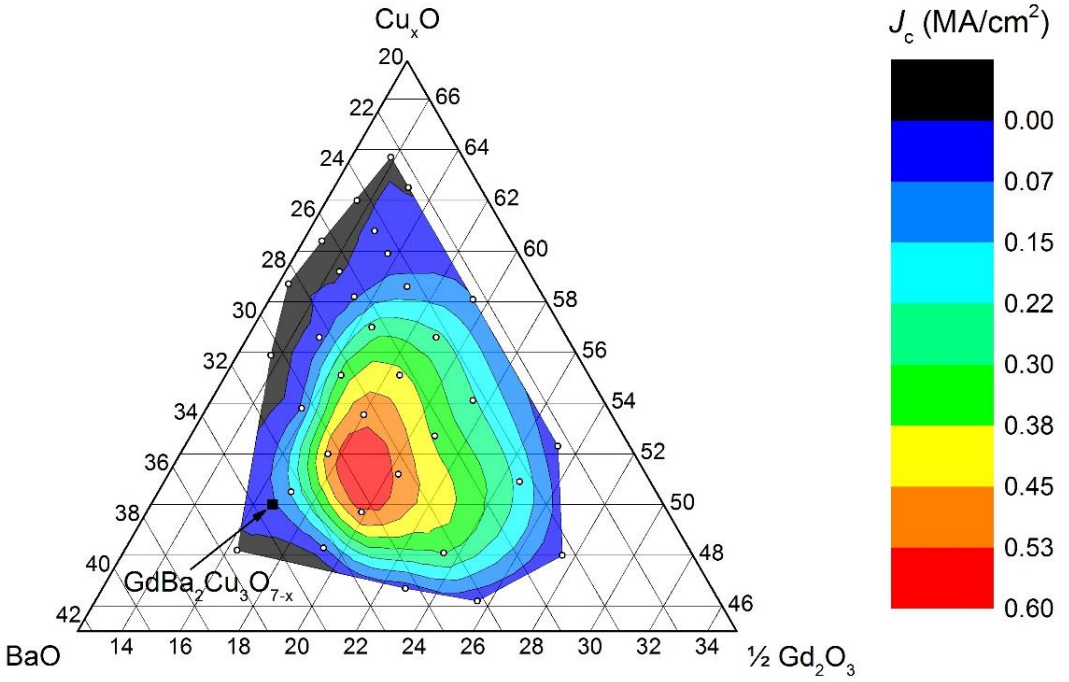

Figure 6. The critical current density distribution of GdBCO films depending on their composition in a ½Gd_2O_3-BaO-Cu_xO ternary phase diagram. White dots correspond to measured samples. Black square indicates the $GdBa_2Cu_3O_{7-x}$ phase.

The critical current density distribution of GdBCO films depending on their stoichiometry is shown in a ternary phase diagram ½Gd_2O_3-BaO-Cu_xO in Fig. 6. J_c reaches in maximum 0.6 MA/cm^2 and is obtained in a circular area centered at a composition of Gd:Ba:Cu = 19.1:29.5:51.4, which means excess of copper and gadolinium compared to $GdBa_2Cu_3O_7$ stoichiometry. Films with such a stoichiometry contain Gd_2O_3 and Cu_xO inclusions, which can be overgrown with the superconducting phase due to the growth nature of GdBCO on ISD-MgO buffered layer [9].

Superconducting films with high critical current density are predominantly formed with an excess of copper and gadolinium compared to $GdBa_2Cu_3O_{7-x}$ indicating a stoichiometry boundary for the growth of structured GdBCO films as Gd ≥ 16.7%, Cu ≥ 49.5% and Ba ≤ 31%. Other boundaries for the epitaxial GdBCO growth are fuzzy, thereby creating a large stoichiometry region for the formation of superconducting films. However, while moving away from the stoichiometry corresponding to the maximum critical current density in the direction of decreasing Ba content, respectively growing Gd and/or Cu content, J_c gradually decreases.

For the growth of structured REBCO films in a deposition area of 20 × 20 cm^2, stoichiometry variations of up to ~ 3% are expected [5]. The stoichiometry region with a critical current density of >75% of the maximum J_c value meets these requirements. For manufacturing one would choose a base stoichiometry that would avoid low Cu and Gd content as well as high Ba content at any time while processing.

4. Conclusion

We have demonstrated the epitaxial growth of the superconducting films by the quantitative electron beam evaporation of the DyBCO and GdBCO powders without employing an oxygen shuttle. The growth parameters match with the Borman diagram, and best crystallinity is achieved at 685°C and an oxygen partial pressure of 1 × 10^{-3} mbar. A critical current density of 0.6 MA/cm^2 was achieved on GdBCO films but the growth rate for high-quality films is limited to 1 Å/s so far. Good

superconducting properties were found within a large stoichiometry region of ~ 3.5% for each element which makes this method suitable for deposition on large areas. These results fulfill the requirements necessary for coated conductor manufacturing, and by abolishing the oxygen shuttle the complexity of the technique is minimized. For economical use, the deposition rate has to be increased, which might be achieved by increasing the background oxygen pressure.

References

[1] Hammond R H and Bormann R 1989 Correlation between the in situ growth conditions of YBCO thin films and the thermodynamic stability criteria *Physica C: Superconductivity and its Applications* **162–164** 703-4

[2] Lee J W, Choi S M, Song J H, Lee J H, Moon S H and Yoo S I 2014 Stability phase diagram of $GdBa_2Cu_3O_{7-\delta}$ in low oxygen pressures *J. of Alloys and Compounds* **602** 78-86

[3] Prusseit W, Sigl G, Nemetschek R, Hoffmann C, Handke J, Lümkemann A and Kinder H 2005 Commercial coated conductor fabrication based on inclined substrate deposition *IEEE Transactions on Appl. Superconductivity* **15** 2608-10

[4] Kinder H, Berberich P, Prusseit W, Rieder-Zecha S, Semerad R and Utz B 1997 YBCO film deposition on very large areas up to 20×20 cm^2 *Physica C: Superconductivity* **282–287** 107-10

[5] Hoffmann C 2003 YBCO-Dauerbeschichtung auf sehr großen Flächen *Technical University of Munich*

[6] Claassen J H, Reeves M E and Soulen R J 1991 A contactless method for measurement of the criticalcurrent density and critical temperature of superconducting films *Rev. Sci. Instrum*. **62** 996

[7] Nelstrop J A G and MacManus-Driscoll J L 2002 Phase stability of erbium barium cuprate, $ErBa_2Cu_3O_{7-x}$ and ytterbium barium cuprate, $YbBa_2Cu_3O_{7-x}$ *Physica C: Superconductivity* **377** 585-94

[8] Hoffmann C, Lümkemann A, Schmatz U, Bauer M, Metzger R, Berberich P and Kinder H 2003 $YBa_2Cu_3O_{7-x}$ deposition of large moving plates for continuous processing *IEEE Transactions on Appl. Superconductivity* **13** 2879-81

[9] Prusseit W, Bauer M, Große V, Semerad R, Sigl G, Dürrschnabel M, Aabdin Z and Eibl O 2012 Working around HTS thickness limitations – towards 1000+ A/cm – Class Coated Conductors *Physics Procedia* **36** 1417-22